

# A Hybrid Atomistic–Continuum Formulation for Unsteady, Viscous, Incompressible Flows

H.S. Wijesinghe<sup>1</sup> and N.G. Hadjiconstantinou<sup>2</sup>

**Abstract:** We present an implicit hybrid atomistic–continuum formulation for unsteady, viscous, incompressible flows. The coupling procedure is derived from a domain decomposition method known as the Schwarz alternating method. A dilute gas impulsive Couette flow test problem is used to verify the hybrid scheme. Finally, a method to reduce computational costs through limited ensemble averaging is presented. The implicit formulation proposed here is expected to be significantly faster than a time explicit approach based on a compressible formulation for the simulation of low speed flows such as those found in micro- and nano-scale devices.

## 1 Introduction and Background

Hybrid atomistic–continuum formulations allow the simulation of complex hydrodynamic phenomena at the nano and micro scales without the prohibitive cost of a fully atomistic approach. Hybrid formulations typically employ a domain decomposition strategy whereby the atomistic model is limited to regions of the flow field where required and the continuum model is used in the remainder of the domain within a single computational framework. Over the years a fair number of unsteady hybrid formulations have been proposed for gases [Eggers and Beylich (1994); Garcia, Bell, Crutchfield, and Alder (1999); Hash and Hassan (1997); Roveda, Goldstein, and Varghese (2000); O’Connell and Thompson (1995); Wadsworth and Erwin (1990, 1992)] and recently for liquids [Delgado and Coveney (2003); Flekkoy, Wagner, and Feder (2000)]. These hybrid formulations are typically based on time explicit flux matching techniques which are natural extensions of control volume integration. In this paper we show that these approaches, while successful when the flow

physics is appropriately compressible, are inefficient when applied to incompressible flow fields [Wijesinghe and Hadjiconstantinou (2004)].

### 1.1 Challenges in Unsteady Incompressible Hybrid Formulations

It is well known that unless special measures are taken, such as pre-conditioning, a compressible continuum formulation should in general be avoided for the solution of incompressible flow fields [Wesseling (2001)]. The timestep for explicit integration of a compressible continuum formulation,  $\Delta t_c$ , scales with the physical time step,  $\Delta t_h = \Delta x_c/U$  (which, in continuum applications, is in balance with the physical time scale  $L/U$ ), according to [Wesseling (2001)],

$$\Delta t_c \leq \frac{M}{1+M} \Delta t_h \quad (1)$$

where  $\Delta x_c$  is the continuum grid spacing,  $L$  and  $U$  are characteristic length and velocity scales and  $M$  is the Mach number. As the Mach number decreases,  $\Delta t_c$  becomes increasingly smaller than  $\Delta t_h$  and the well-known stiffness problem arises whereby the computational efficiency of the numerical scheme degrades due to disparity of time scales in the system of governing equations. Moreover the accuracy of the compressible solution degrades because the magnitude of fluxes in the original equations approach the corresponding terms due to numerically added artificial viscosity [Wong, Darmofal, and Peraire (2001)].

In the hybrid case, the atomistic integration time step,  $\Delta t_p$ , also needs to be considered.  $\Delta t_p$  is at most of the order of  $\Delta t_c$  (for some cases in gases when  $\Delta x \lesssim \lambda$ ) and in most cases significantly smaller (especially in liquids). These considerations make unsteady incompressible problems particularly challenging since as  $L$  grows, the separation between  $\Delta t_p$  and  $\Delta t_h$  makes the explicit

<sup>1</sup> Department of Aeronautics/Astronautics, Massachusetts Institute of Technology

<sup>2</sup> Department of Mechanical Engineering, Massachusetts Institute of Technology, 77 Massachusetts Ave., Cambridge, MA 02139, USA.

integration of the atomistic subdomain to the time of interest increasingly expensive and eventually infeasible. These issues have been addressed for *steady* incompressible problems [Hadjiconstantinou and Patera (1997); Hadjiconstantinou (1999)] with the use of iterative methods that lead to convergence to the global steady state solution without the need for explicit integration of the atomistic subdomain to this solution. Time explicit coupling schemes should therefore be avoided for steady problems. In unsteady flows however, since the interest lies in the transient solution, iterative steady state methods cannot be used. Innovative integrative frameworks which can coarse grain the time integration of the atomistic subdomain may alleviate some of these problems in the future.

In this paper we assume that  $L$  is sufficiently small such that explicit integration of the atomistic subdomain to the global time of interest is possible. Under these conditions, explicit and implicit coupling techniques based on incompressible formulations offer advantages compared to the commonly used time explicit flux matching based on the compressible continuum (control volume) formulation. An example of an implicit technique is introduced next and is the subject of the remainder of this paper. An explicit technique based on the incompressible formulation was presented in [O'Connell and Thompson (1995)].

## 1.2 An Implicit Coupling Technique

Here we explore the use of a coupling method more in tune with the physics of the incompressible flow field. The approach considered is an extension of the Schwarz alternating method [Han and Atluri (2002, 2003); Lions (1988)] used to provide hybrid descriptions of steady state liquid systems [Hadjiconstantinou and Patera (1997)] and demonstrated more recently for a 2-dimensional driven cavity gas flow [Wijesinghe and Hadjiconstantinou (2002)] and for microfluidic design [Aktas and Aluru (2002)]. In the Schwarz method, coupling is achieved in an implicit sense through the successive exchange of state variables (Dirichlet boundary conditions) across an overlap region. The Schwarz procedure is guaranteed to converge for elliptic problems [Lions (1988)], and has recently been shown to converge for finite Reynolds numbers [Liu (2001)].

In the current paper we choose to focus our atten-

tion on dilute gas systems where the Navier-Stokes description fails as the characteristic length scale of interest decreases [Hadjiconstantinou and Simek (2002); Hadjiconstantinou (2002, 2003); Hadjiconstantinou and Simek (2003)]. The hybrid formulation introduced here is nonetheless equally applicable to liquids. As explained in [Wijesinghe and Hadjiconstantinou (2004)], in the case of liquids the only significant modification required is a reliable boundary condition imposition method in the atomistic subdomain for which progress has been made recently [Delgado and Coveney (2003); Flekkoy, Wagner, and Feder (2000); Li, Liao, and Yip (1999)].

The Schwarz method offers two advantages compared to time explicit coupling approaches based on flux matching. First, the time scale decoupling properties of the approach are manifested by the ability to couple only at the time where solutions are required. This not only allows the use of optimal time steps in each subdomain but also the use of acceleration methods such as the limited ensemble approach developed here to gain an efficiency advantage.

The second advantage arises from the fact that Schwarz coupling using state variables provides cost savings over traditional flux based coupling schemes. Flux based formulations suffer from adverse signal to noise ratios in connection with the averaging required for imposition of boundary conditions from the atomistic subdomain to the continuum subdomain. In the case of an ideal gas and low speed flows it has been shown [Hadjiconstantinou, Garcia, Bazant, and He (2003)] that, for the same number of samples, flux (shear stress, heat flux) averaging exhibits relative noise  $E_f$  which scales as

$$E_f \approx \frac{E_{sv}}{Kn} \quad (2)$$

where  $E_{sv}$  is the relative noise in the corresponding state variable (velocity, temperature) which varies as  $1/\sqrt{(\text{number of samples})}$ . Here  $Kn = \lambda/L$  is the Knudsen number based on the characteristic length scale of the transport gradients,  $L$ , and  $\lambda$  is the mean free path which is expected to be much smaller than  $L$  since, by assumption, a continuum subdomain is present. It thus appears that coupling using fluxes will be significantly disadvantaged in this case since  $1/Kn^2$  times the number of samples required by state-variable averaging is

required to achieve comparable variance reduction in the matching region (where  $Kn \ll 1$ ).

The disadvantage of the Schwarz method is the need for  $O(10)$  iterations for convergence. This computational cost can however easily be recuperated through the efficiency gained from the above advantages, especially in higher dimensions; the number of iterations required is fairly insensitive to the dimensionality of the problem.

The outline of the paper is as follows. First, the unsteady Schwarz coupling approach is described and evaluated using a continuum–continuum test problem. A strategy for reducing the computational cost of unsteady schemes using a limited ensemble averaging technique is then presented. Finally a hybrid atomistic–continuum formulation for an unsteady impulsively driven Couette flow test problem is presented.

## 2 Unsteady Schwarz Coupling

The Schwarz alternating method can be extended to couple time unsteady flows to some time  $t^n$  by exchanging boundary condition information similar to steady flow coupling [Lions (1988)]. As shown schematically in Figure 1, an overlap region between the subdomains facilitates information exchange in the form of Dirichlet boundary conditions. A continuum solution based on the unsteady equations of motion is first obtained using boundary conditions taken from the atomistic subdomain solution. At the first iteration this latter solution can be a guess. An atomistic solution is then found by integrating the atomistic subdomain to time  $t^n$  using boundary conditions taken from the continuum subdomain. This exchange of boundary conditions corresponds to a single Schwarz iteration. This process is repeated to convergence. The converged solution at  $t^n$  forms the initial condition for subsequent Schwarz iterations to advance the solution to time level  $t^{n+1}$ . The unsteady Schwarz scheme still allows for time scale decoupling; each subdomain can be advanced at the local most favorable time step and the choice of  $t^{n+1}$  is arbitrary. The computational cost of performing multiple Schwarz iterations per time level is thus partially offset by the ability to implicitly advance to the time of interest without the need for explicit coupling at previous times. This also allows for acceleration techniques such as the one we describe be-

low. Note that the steady Schwarz method can be considered as the special case of the unsteady Schwarz method for  $t^n \rightarrow \infty$  in the presence of a steady state.

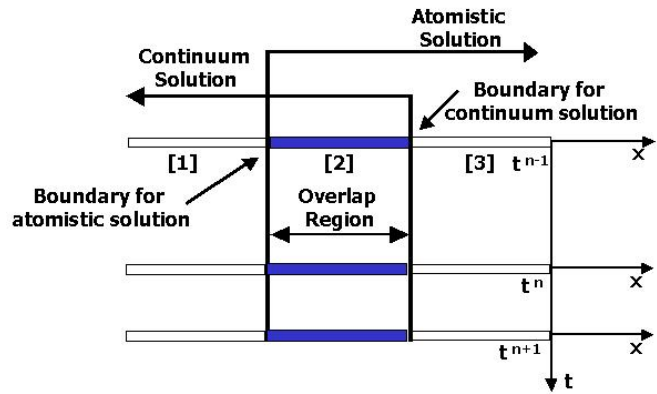


**Figure 1** : Illustration of the unsteady Schwarz coupling method in one spatial dimension.

Implementation of the unsteady Schwarz method requires 2 additional constructs not present in the steady scheme; the first is ensemble averaging of the unsteady atomistic subdomain solution and the second is time interpolation of solutions between atomistic and continuum subdomains to allow for different time steps in these subdomains.

### 2.1 Particle Ensembles

Integration of the continuum subdomain in hybrid methods is achieved by receiving boundary data (state or flux variables) from the atomistic subdomain. This data is typically obtained by averaging the atomistic solution field over a number of realizations (time or ensemble members). In unsteady flows, unless the flow is evolving very slowly, time averaging has the result of smearing the solution and is thus avoided; ensemble averaging is therefore used instead. Additionally, due to their low characteristic speeds, incompressible flows suffer from high relative statistical error (defined here as the one standard deviation of the statistical fluctuation in estimating the mean value of a quantity over the mean value of the same quantity [Hadjiconstantinou, Garcia, Bazant, and He (2003)]). For this reason ensemble averaging and large numbers of particles per cell are an

integral part of atomistic simulations of unsteady low speed flows.

### 2.2 Time Interpolation

A distinctive advantage of steady Schwarz coupling is its ability to decouple time scales [Wijesinghe and Hadjiconstantinou (2002)]; the time step for the continuum subdomain  $\Delta t_c$  is often larger than the time step for the atomistic subdomain  $\Delta t_p$ . Similar time scale decoupling is also possible using unsteady Schwarz coupling. For the case where  $\Delta t_c > \Delta t_p$ , the boundary values from the continuum solutions must be interpolated to the atomistic subdomain as shown schematically in Figure 2, to ensure the atomistic subdomain solution has the most accurate boundary conditions during advance to any time level  $t^{n+1}$ . Note that during time advance of the continuum subdomain, direct imposition of the atomistic subdomain boundary condition is possible provided the continuum subdomain time step is an integer multiple of the atomistic subdomain time step.

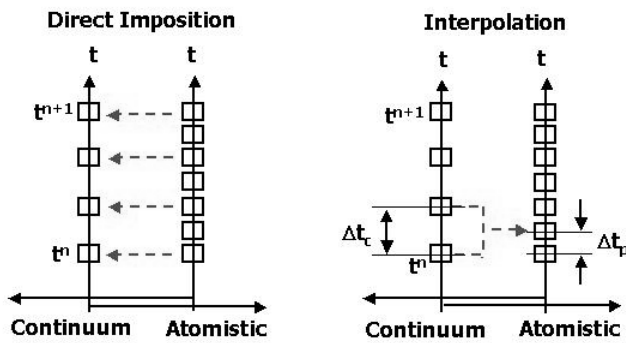


Figure 2 : Interpolation of boundary conditions.

The effectiveness of linear time interpolation of the continuum boundary condition is assessed next using a hybrid (unsteady Schwarz) continuum–continuum scheme. The continuum–continuum test problem helps evaluate the time interpolation routines independently of the ensemble averaging required for an atomistic–continuum formulation and hence in the absence of statistical fluctuations which make quantitative comparison difficult.

### 2.3 Method Verification Using a Continuum–Continuum Problem

The impulsive Couette flow shown in Figure 3 is used as a test problem. The wall at  $x = L$  moves with velocity  $V_0$  at time  $t = 0$  while the wall at  $x = 0$  is held stationary. The hybrid scheme consists of 2 continuum subdomains *I* and *II* extending between  $0 \leq x \leq b$  and from  $a \leq x \leq L$  respectively with overlap width  $h$ .

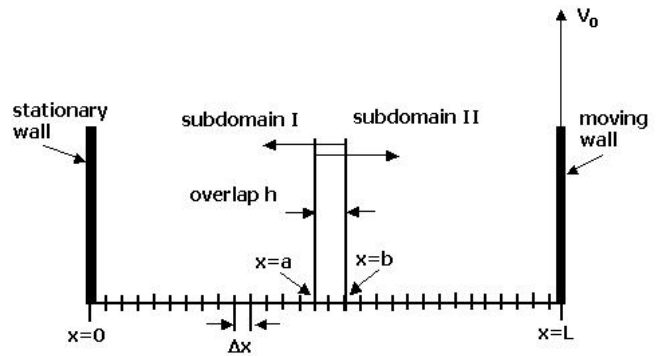


Figure 3 : Computational domain for the impulsively started Couette flow test problem.

The resulting flow is obtained by solution of a diffusion equation for  $y$ -momentum,

$$\frac{\partial v}{\partial t} - \nu \frac{\partial^2 v}{\partial x^2} = 0 \quad x \in (0, L), t \in (0, T) \quad (3)$$

where  $\nu = \mu/\rho$  is the kinematic viscosity. This equation can be solved numerically using an implicit backward difference scheme (i.e. Backward Euler),

$$\partial_{t,\Delta t} v_i^n - \partial_{x,\Delta x}^2 v_i^n = 0 \quad (4)$$

where,

$$\partial_{t,\Delta t} v(x, t) = \frac{v(x, t) - v(x, t - \Delta t)}{\Delta t} \quad (5)$$

$$\partial_{x,\Delta x}^2 v(x, t) = \frac{v(x - \Delta x, t) - 2v(x, t) + v(x + \Delta x, t)}{\Delta x^2} \quad (6)$$

Here  $\Delta t$  is the time step and  $\Delta x$  is the spatial discretization. Equation (4) is used in both subdomains *I* and *II*. In

Property	Value
Domain length $L$	$2.00 \times 10^{-6}$ m
Kinematic viscosity	$1.1688665 \times 10^{-5}$ m <sup>2</sup> /s
Characteristic time $t_0$	$L^2/\nu = 3.4221188 \times 10^{-7}$ s
Wall velocity $V_0$	30 m/s
Non-dimensional overlap width $h/L$	0.03
Non-dimensional boundary $a/L$	0.47
Non-dimensional boundary $b/L$	0.50
Subdomain $I$ non-dimensional time step	$\Delta t_I = 2.922 \times 10^{-4}$
Subdomain $I$ non-dimensional grid size	$\Delta x_I = 0.01$
Subdomain $II$ non-dimensional time step	$\Delta t_{II} = 2.922 \times 10^{-5}$
Subdomain $II$ non-dimensional grid size	$\Delta x_{II} = 0.01$
Schwarz iterations / $\Delta t_I$	10

**Table 1 :** Properties of hybrid continuum–continuum scheme used for the impulsive Couette flow test problem.

this test problem, subdomain  $II$  is advanced at 1/10th the time step of subdomain  $I$ . The LHS boundary condition for subdomain  $II$ ,  $v_{II}(a, t)$  is linearly interpolated from the subdomain  $I$  solution as follows,

$$v_{II}(a, t^k) = v_I(a, t^i) + \frac{(k - pi)}{p} (v_I(a, t^{i+1}) - v_I(a, t^i))$$

where  $i$  is given by  $t^i < t^k \leq t^{i+1}$  (7)

Here  $p = \Delta t_I / \Delta t_{II}$ , and  $i, k$  are the indices of the time step used in subdomains  $I$  and  $II$  respectively. The RHS boundary condition for subdomain  $I$ ,  $v_I(b, t)$  is obtained by direct imposition of the subdomain  $II$  solution as follows,

$$v_I(b, t^i) = v_{II}(b, t^k) \text{ where } k = pi \quad (8)$$

Additional parameters for the impulsive Couette flow test are listed in Table 1.

The velocity profiles predicted by the hybrid scheme are plotted in Figure 4 together with a solution obtained by numerical integration of Equation (3) in a single domain with  $\Delta x/L = 0.01$  and  $\Delta t/t_0 = 2.922 \times 10^{-5}$  (referred to here as the exact solution). The hybrid scheme velocity profiles are in good agreement with the exact solution. The number of Schwarz iterations for convergence varies between 3 and 8 as  $h/L$  varies between 0.02 and 0.04, with larger number of iterations required for smaller overlaps.

The convergence of the velocity profile at time  $t/t_0 = 0.11688$  to the exact solution as a function of Schwarz iterations and interpolation scheme is plotted in Figure 5. The linearly interpolated boundary condition solution converges after approximately 5 Schwarz iterations. The velocity solution using stepwise boundary condition interpolation (i.e.  $v_{II}(a, t^k) = v_I(a, t^{i+1})$  for  $pi < k \leq p(i + 1)$ ) also converges but with larger deviation. The use of equal time steps  $\Delta t/t_0 = 2.922 \times 10^{-5}$ s in both subdomains, i.e. where direct boundary condition imposition is possible between subdomains  $I \rightarrow II$  and  $II \rightarrow I$  shows the best performance. This final result verifies consistency of the unsteady Schwarz coupling when no time step difference between the subdomains is exists. While use of equal time steps in both subdomains results in greater accuracy, this must be weighed with the benefit of reduced hybrid simulation cost through time step decoupling. Linear interpolation of the boundary condition provides a reasonable balance between the two constraints in this case. Application of unsteady Schwarz coupling to hybrid atomistic–continuum schemes is demonstrated next.

### 3 Application to Atomistic–Continuum Systems

We now proceed to apply the unsteady Schwarz method to atomistic–continuum systems. The atomistic model in this paper is the direct simulation Monte Carlo method [Bird (1994)]. The DSMC method is based on the assumption that a small number of representative “computational particles” can accurately capture the

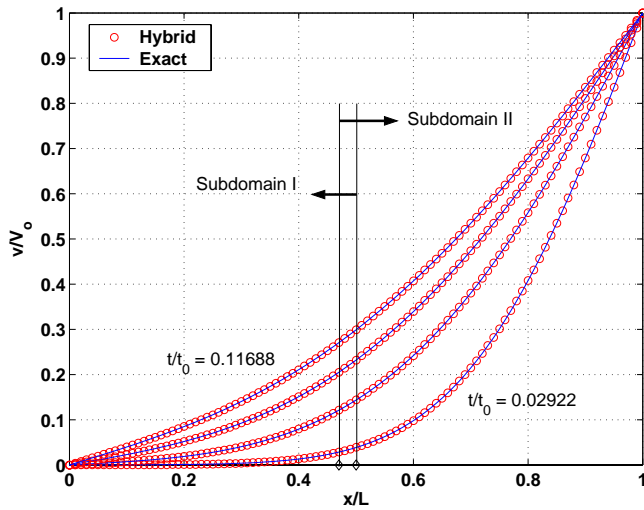


**Figure 4 :** Comparison of the hybrid continuum-continuum solution for the impulsively driven Couette test problem with the exact solution. Overlap  $h/L = 0.03$ . Profiles are shown for non-dimensional times  $t/t_0 = 0.02922$  to  $t/t_0 = 0.11688$  in steps of 0.02922.

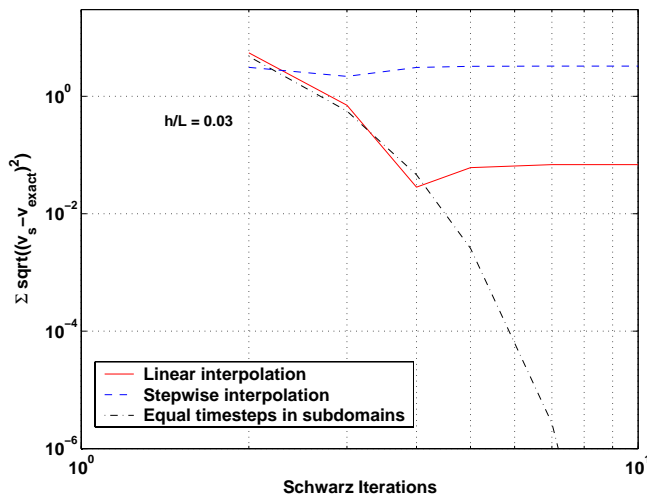


**Figure 5 :** Convergence of the hybrid continuum-continuum velocity profile at  $t/t_0 = 0.11688$  as a function of number of Schwarz iterations and boundary condition interpolation scheme. The summation is taken over the complete domain.

bulk hydrodynamics of a complete system of gas atoms or molecules. In DSMC the particle positions and velocities ( $\mathbf{r}_i, \mathbf{v}_i, i = 1 \dots N$ ) are advanced in time by a two-step process of advection and collision which corresponds to a splitting method of solution for the underlying Boltzmann equation. Particle advection is ballistic with time step  $\Delta t_p$  chosen to be a fraction of the mean collision time [Hadjiconstantinou (2000)]. Collisions are performed between randomly chosen particle pairs within small cells of size  $\Delta x_p$  [Alexander, Garcia, and Alder (2000)]. This approach has been shown to produce correct solutions to the Boltzmann equation in the limit  $\Delta x_p, \Delta t_p \rightarrow 0$  [Wagner (1992)]. Argon gas (atomic mass  $m = 6.63 \times 10^{-26}$  kg and hard sphere diameter  $\sigma = 3.66 \times 10^{-10}$  m) was used for all simulations.

### 3.1 Acceleration Using a Limited Number of Ensembles

In this Section we develop an acceleration scheme that takes advantage of the time scale decoupling properties of the Schwarz method to reduce the computational cost associated with ensemble averaging the atomistic subdomain solution. The idea behind this method is that a large number of ensemble members is only needed for noise reduction purposes whereas the hydrodynamic behavior of the system is present in *any* of the ensemble members albeit in a noisy form. Thus, since the coupling procedure used here allows for a large gap between sampling times (sampling is required only when matching occurs, which can be as infrequent as only once in the calculation) it is natural to attempt to use a large number of ensembles only during the sampling phase. This can be achieved by noting that the decorrelation time between different calculations is small compared to the hydrodynamic time scale (especially for large problems). Thus if a small number of ensemble members are used for the majority of the time integration and from these systems a larger amount of systems are generated by perturbation at a time which allows for decorrelation, a full decorrelated sample will exist when required without integrating this full ensemble through time. In the case of our DSMC calculation sufficiently perturbed systems can be generated by simply changing the random number seed while using the same initial configuration.

In our nomenclature, in the standard non-accelerated

unsteady Schwarz coupling approach  $N_E^{max}$  particle ensemble members are created and advanced through each time interval  $t^n \rightarrow t^{n+1}$ . On the other hand, according to the approach proposed here we split the ensemble creation within a single time interval  $t^n \rightarrow t^{n+1}$  into 2 stages, i.e.  $N_{E1}^{max}$  ensemble members for simulation time  $t^n \rightarrow t^{n+\delta}$  and  $N_{E2}^{max}$  ensemble members for time  $t^{n+\delta} \rightarrow t^{n+1}$  such that,

$$N_{E1}^{max}(t^{n+1} - t^{n+\delta})/\Delta t_p + N_{E2}^{max}(t^{n+\delta} - t^n)/\Delta t_p < N_E^{max}(t^{n+1} - t^n)/\Delta t_p \quad (9)$$

$$N_{E1}^{max} < N_E^{max} \quad (10)$$

where  $\Delta t_p$  is the time step of the atomistic subdomain simulation and  $0 < \delta < 1$ . Note that  $N_{E2}^{max}$  can equal  $N_E^{max}$  to allow the same degree of error reduction in the final solution at time  $t^{n+1}$  as we had in the implementation in the previous Section.

The computation cost reduction of the unsteady Schwarz method using limited ensembles in this manner is dependent on the values of  $\delta$  and  $N_{E1}^{max}$  required to maintain accuracy. Results from an initial analysis of the method using a fully atomistic simulation of an impulsive Couette flow are shown in Figure 6. For these tests  $N_{E2}^{max} = 2000$  and  $\delta$  is chosen such that  $(t^{n+1} - t^{n+\delta})/\Delta t_p = (t^{n+\delta} - t^n)/\Delta t_p = 500$  DSMC time steps. This provides a  $26.9\tau$  decorrelation time before sampling of the atomistic solution. Good comparison is obtained for the  $N_{E1}^{max} = 100$  simulation. The reduction in error as a function of  $N_{E1}^{max}$  is further plotted in Figure 7 which shows a slow decay with  $N_{E1}^{max}$  which indicates that a small number of ensembles is required to carry the dynamics forward in time, i.e.,  $N_{E1}^{max}$  should be kept as small as possible. The choice of parameters for this test using limited ensemble acceleration results in a speed-up of 1.95 over a non-accelerated fully atomistic unsteady simulation. Clearly, the longer  $t^{n+1} - t^n$  the larger the savings since  $\delta$  is associated with the decorrelation time which does not depend on the system size or time of interest. The limited ensemble approach is incorporated within an unsteady hybrid scheme applied to an impulsive Couette flow test problem next.

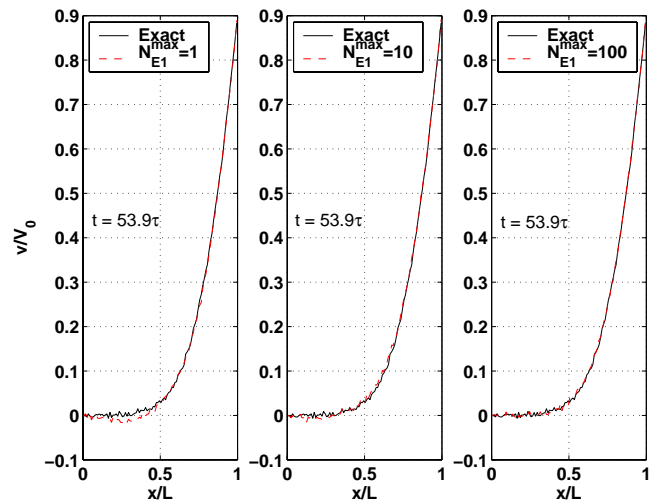


**Figure 6** : Comparison of limited ensemble acceleration using varying number of  $N_{E1}^{max}$  ensembles. The figure shows the velocity profile at  $t = 53.9\tau$  for a fixed  $N_{E1}^{max} = 2000$ .  $\tau = 1.8559 \times 10^{-10}$ s is the characteristic collision time.

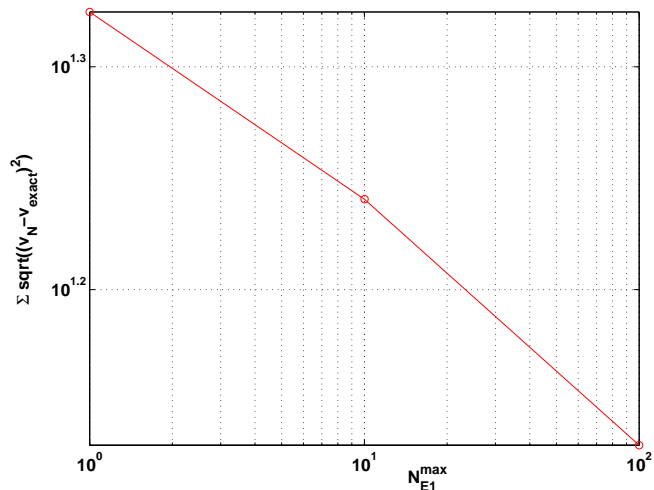


**Figure 7** : Error reduction of limited ensemble acceleration as a function of  $N_{E1}^{max}$ . The summation is taken over the complete domain.

Property	Value
Total domain width $L$	$4 \times 10^{-6}$ m
Wall velocity $V_0$	30 m/s
Kinematic viscosity $\nu$	$1.1688665 \times 10^{-5}$ m <sup>2</sup> /s
Characteristic collision time $\tau$	$1.8559 \times 10^{-10}$ s
Continuum subdomain width $L_c/L$	0.9275
Continuum nodes in $L_c$	186
Continuum time step $\Delta t_c/\tau$	0.5388
Atomistic subdomain width $L_a/L$	0.075
DSMC cells in $L_a$	15
No. of particles in each cell	2000
DSMC time step $\Delta t_p$	0.05388
No. of ensembles $N_{E1}^{max}$	100
No. of ensembles $N_{E2}^{max}$	2000
DSMC time steps per ensemble	500 for both $N_{E1}^{max}$ and $N_{E2}^{max}$
Non-dimensional reservoir region width	0.01
Overlap region width $h/L$	0.0025
Schwarz iterations per time step	10

**Table 2** : Simulation parameters for the hybrid impulsive Couette flow test problem using accelerated unsteady Schwarz coupling.

### 3.2 Impulsive Couette Flow Test Problem

A hybrid atomistic–continuum scheme using unsteady Schwarz coupling is verified in this section for the 1–dimensional impulsive Couette flow test problem shown in Figure 3. The subdomains  $I$  and  $II$  correspond to the continuum and atomistic subdomains respectively. The continuum solution is obtained by solving Equation (3) for the  $y$ –momentum diffusion using the implicit backward difference scheme detailed in Equation (4). The atomistic subdomain is solved using DSMC.

The imposition of continuum boundary conditions on the atomistic subdomain is facilitated by a particle reservoir extending from  $x/L = 0.915$  to  $x/L = 0.925$ . Particles are created in the reservoir with a uniform spatial distribution in the  $x$ –coordinate direction and a velocity drawn from a Chapman–Enskog distribution [Garcia and Alder (1998)]. The mean and gradient of velocity ( $v, \partial v/\partial x$ ) used to generate the Chapman–Enskog distribution is obtained by linear time interpolation according to Equation (7) followed by linear spatial interpolation between the continuum nodes. Imposition of the atomistic boundary conditions on the continuum subdomain follows the use of overlapping continuum nodes and DSMC cell cen-

ters. Direct imposition is possible here as the continuum time step is chosen to be an integer multiple of the DSMC time step. Parameters for the unsteady simulation are listed in Table 2.

Limited ensemble acceleration can be incorporated within the hybrid scheme with minor modifications. The ensemble creation loop is split into 2 stages during advance of the atomistic solution calculated by DSMC; we utilize two families of particle ensembles that consist of  $N_{E1}^{max}$  and  $N_{E2}^{max}$  members respectively where  $N_{E2}^{max} > N_{E1}^{max}$ . The  $N_{E2}^{max}$  members are created by splitting off an additional ( $N_{E2}^{max} - N_{E1}^{max}$ ) members with different random number seeds at time  $t^{n+\delta}$  from the  $N_{E1}^{max}$  original ensembles as shown graphically in Figure 8. Ensemble creation in this manner is repeated for  $N_s^{max}$  Schwarz iterations in the time interval  $t^n$  to  $t^{n+1}$ . At each Schwarz iteration, updated boundary conditions are exchanged to achieve a converged solution at time level  $t^{n+1}$ . At the final Schwarz iteration  $N_s^{max}$ , the  $N_{E2}^{max}$  ensemble members are averaged to yield the time level  $t^{n+1}$  flow solution. A limited subset of the  $N_{E2}^{max}$  ensemble members are then advanced forward as the new  $N_{E1}^{max}$  ensemble family for the next time interval. The velocities of these new  $N_{E1}^{max}$

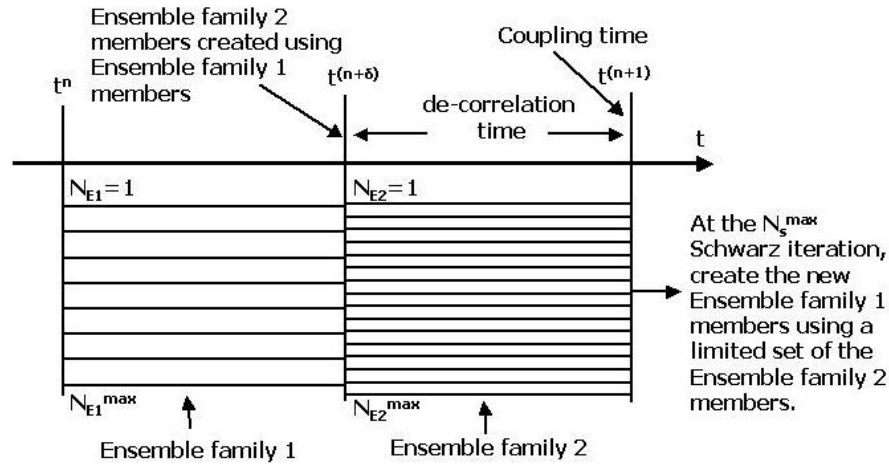


**Figure 8 :** Graphical illustration of the limited ensemble acceleration approach.

members are initialized to the  $t^{n+1}$  ensemble-averaged solution. The ensemble creation process is then repeated for the next time interval.

In this simulation 10 Schwarz iterations are used to couple the solution at every  $53.9\tau$ . While this choice is driven by the need to provide sufficient decorrelation time before sampling of the  $N_{E2}^{max}$  ensembles, it also highlights the versatility of the hybrid Schwarz coupling to match solutions at arbitrary times.

The results from the accelerated unsteady hybrid scheme are shown in Figure 9. Good comparison is obtained with a fully atomistic solution. The simulation cost of this scheme is compared to a fully atomistic scheme and a non-accelerated unsteady Schwarz scheme in Table 3. The use of limited ensemble acceleration has helped reduce the total simulation cost of the unsteady hybrid scheme to a total of more than a factor of 2 despite the fact that the parameter choices for  $\delta$  and  $N_{E1}^{max}$  have not been optimized in any way. Of course hybrid methods are capable of significantly larger speed-ups. The reason for the modest speed-up observed here is two fold. First, the problem is one-dimensional. Second, the problem was chosen small enough such that a fully atomistic solution would be feasible for comparison purposes. For problems of practical interest we expect the volume of the continuum region to be larger thus leading to significantly larger savings. Larger continuum domain volumes may result from larger systems or simply higher dimensionality. The importance of dimensionality can be demonstrated by considering that the speed-up in a two-dimensional problem of the same approximate linear dimensions as the above test problem would be of  $O(20)$ ; for a three-dimensional problem it would be of  $O(200)$ . These savings are possible since the number of iterations to convergence for the Schwarz method is insensitive to the dimensionality of the problem. Larger linear system dimensions bring additional savings because the decorrelation timescale becomes a smaller fraction of the characteristic system timescale.

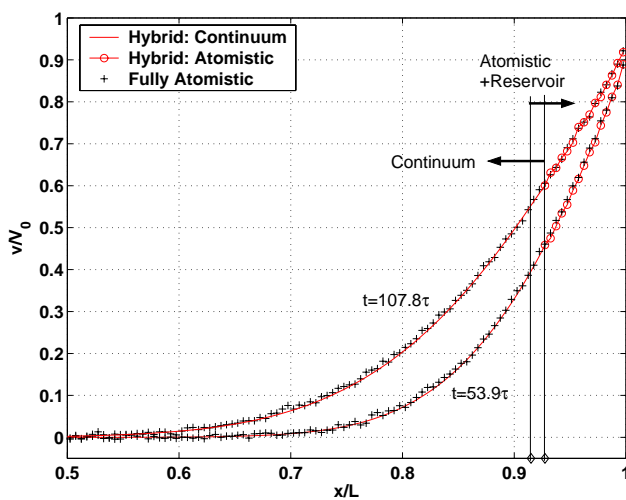


**Figure 9 :** Comparison of limited ensemble accelerated unsteady hybrid scheme for impulsive Couette flow with fully atomistic solution.  $\tau = 1.8559 \times 10^{-10}$ s is the mean collision time.

Property	Atomistic	Hybrid	Hybrid (accelerated)
Atomistic subdomain width $L_a$	4.00 $\mu\text{m}$	0.3 $\mu\text{m}$	0.3 $\mu\text{m}$
Ensembles $N_E^{max}$	2000	2000	$N_{E1}^{max} = 100, N_{E2}^{max} = 2000$
DSMC time steps $N_{m1}^{max}$	1000	1000	500 for both $N_{E1}^{max}$ and $N_{E2}^{max}$
Schwarz iterations $N_s^{max}$	0	10	10
Cost ( $L_a \times N_{m1}^{max} \times N_E^{max} \times N_s$ )	$8 \times 10^6$	$6 \times 10^6$	$3.15 \times 10^6$
Speed-up	-	1.33	2.54

**Table 3** : Comparison of simulation cost.

#### 4 Conclusions

In general, large savings can be achieved by hybrid methods in more than one dimension where the volume of the continuum subdomain grows fast with the linear dimensions of the problem [Aktas and Aluru (2002)]. In this paper the Schwarz alternating method for hybrid atomistic–continuum coupling has been extended to couple unsteady incompressible flows. Tests for an impulsively driven Couette flow highlight the versatility of this coupling approach to advance solutions implicitly in time by exchanging Dirichlet boundary conditions at arbitrary times. A technique which uses limited ensemble averaging of the atomistic solution has also been developed to realize computational savings over a standard ensemble process while maintaining the same variance reduction. Since a large number of ensembles need only be run for a small fraction of the calculation using this approach, large savings can be achieved in cases of practical interest where the global time scales of evolution will be long compared to the atomistic collision (decorrelation) time. Note that if the timescale between solutions is not significantly longer than the decorrelation timescale, an explicit coupling method, again based on the incompressible formulation may be preferable. The current method is *estimated* to be  $O(10)$  times faster than a time explicit coupling technique based on the compressible formulation for the particular test problem solved here. This estimate does not include the savings from using a simple incompressible solver in the continuum subdomain compared to a compressible formulation which would be limited by CFL time step considerations. In the future we plan to investigate the relation between the cost of flux and state property averaging in liquids. As shown in this paper this relation has a large bearing on the type of coupling algorithm used.

**Acknowledgement:** This work has been supported by the Lawrence Livermore National Laboratory. The authors would like to thank B. J. Alder and A. T. Patera for helpful comments and discussions.

#### References

- Aktas, O.; Aluru, N. R.** (2002): A Combined Continuum/DSMC Technique for Multiscale Analysis of Microfluidic Filters, *Journal of Computational Physics*, **178**, pp. 342–372.
- Alexander, F. J.; Garcia, A. L.; Alder, B. J.** (2000): Cell Size Dependence of Transport Coefficients in Stochastic Particle Algorithms, *Physics of Fluids*, **10**, p. 1540, (1998); erratum, *Physics of Fluids*, **12**, p. 731.
- Bird, G. A.** (1963): Approach to Translational Equilibrium in a Rigid Sphere Gas, *Physics of Fluids*, **6**, pp. 1518–1519.
- Bird, G. A.** (1994): *Molecular Gas Dynamics and the Direct Simulation of Gas Flows*, Clarendon Press, Oxford.
- Delgado–Buscalioni, R.; Coveney, P. V.** (2003): Continuum–Particle Hybrid Coupling for Mass, Momentum and Energy Transfers in Unsteady Fluid Flow, *Physical Review E*, **67**, No. 4.
- Eggers, J.; Beylich, A.** (1994): New algorithms for application in the direct simulation Monte Carlo method, *Progress in Astronautics and Aeronautics*, **159**, pp. 166–173.
- Fallavollita, M. A.; Baganoff, D.; McDonald, J. D.** (1993): Reduction of Simulation Cost and Error for Particle Simulations of Rarefied Flows, *Journal of Computational Physics*, **109**, pp. 30–36.
- Flekkoy, E. G.; Wagner, G.; Feder, J.** (2000): Hybrid model for combined particle and continuum dynamics, *Europhysics Letters*, **52**, pp. 271–276.

- Garcia, A. L.; Alder, B. J.** (1998): Generation of the Chapman Enskog Distribution, *Journal of Computational Physics*, **140**, pp. 66–70.
- Garcia, A. L.; Bell, J. B.; Crutchfield, W. Y.; Alder, B. J.** (1999): Adaptive Mesh and Algorithm Refinement Using Direct Simulation Monte Carlo, *Journal of Computational Physics*, **54**, pp. 134–155.
- Hadjiconstantinou, N. G.; Patera, A. T.** (1997): Heterogeneous Atomistic-Continuum Representations for Dense Fluid Systems, *International Journal of Modern Physics C*, **8**, pp. 967–976.
- Hadjiconstantinou, N. G.** (1999): Hybrid Atomistic-Continuum Formulations and the Moving Contact-Line Problem, *Journal of Computational Physics*, **154**, pp. 245–265.
- Hadjiconstantinou, N. G.** (2000): Analysis of discretization in the direct simulation Monte Carlo, *Physics of Fluids*, **12**, pp. 2634–2638.
- Hadjiconstantinou, N. G.; Simek, O.** (2002): Constant-Wall-Temperature Nusselt Number in Micro and Nano-Channels, *Journal of Heat Transfer*, **124**, 356-364.
- Hadjiconstantinou, N. G.** (2002): Sound wave propagation in transition-regime micro- and nanochannels, *Physics of Fluids*, **14**, 802-809.
- Hadjiconstantinou, N. G.** (2003): Comment on Cercignani's second-order slip coefficient, *Physics of Fluids*, **15**, 2352-2354.
- Hadjiconstantinou, N. G.; Simek, O.** (2003): Sound propagation at small scales under continuum and non-continuum transport, *Journal of Fluid Mechanics*, **488**, 399-408.
- Hadjiconstantinou, N. G.; Garcia, A. L.; Bazant, M. Z.; He, G.** (2003): Statistical Error in Particle Simulations of Hydrodynamic Phenomena, *Journal of Computational Physics*, **187**, pp. 274–297.
- Han, Z. D.; Atluri, S. N.** (2002): SGBEM (for Cracked Local Subdomain)–FEM (for uncracked global Structure) Alternating Method for Analyzing 3D Surface Cracks and Their Fatigue-Growth, *CMES: Computer Modeling in Engineering & Sciences*, **3**, No. 6, pp. 699–716.
- Han, Z.D.; Atluri, S.N.** (2003): On simple formulations of weakly-singular tBIE&dBIE, and Petrov-Galerkin approaches, *CMES: Computer Modeling in Engineering & Sciences*, **4**, No. 1, pp. 5–20.
- Hash, D.; Hassan, H.** (1997): Two-Dimensional Coupling Issues of Hybrid DSMC/Navier Stokes Solvers, *AIAA Paper 97-2507*.
- Li, J.; Liao, D.; Yip, S.** (1999): Nearly exact solution for coupled continuum/MD fluid simulation, *Journal of Computer-Aided Materials Design*, **6**, pp. 95–102.
- Lions, P. L.** (1988): On the Schwarz alternating method. I., *First International Symposium on Domain Decomposition Methods for Partial Differential Equations*, Eds. R. Glowinski, G. Golub, G. Meurant and J. Periaux, 1–42, SIAM, Philadelphia.
- Liu, S. H.** (2001): On Schwarz Alternating Methods For The Incompressible Navier-Stokes Equations, *Siam Journal of Scientific Computing*, **22**, No. 6, pp. 1974–1986.
- O'Connell, S. T.; Thompson, P. A.** (1995): Molecular dynamics-continuum hybrid computations: A tool for studying complex fluid flows, *Physical Review E*, **52**, pp. R5792–R5795.
- Roveda, R.; Goldstein, D. B.; Varghese, P. L.** (2000): Hybrid Euler/direct simulation Monte Carlo calculation of unsteady slit flow, *Journal of Spacecraft and Rockets*, **37** No. 6, pp. 753–760.
- Wadsworth, D. C.; Erwin, D. A.** (1990): One-Dimensional Hybrid Continuum/Particle Simulation Approach for Rarefied Hypersonic Flows, *AIAA Paper 90-1690*.
- Wadsworth, D. C.; Erwin, D. A.** (1992): Two-Dimensional Hybrid Continuum/Particle Simulation Approach for Rarefied Hypersonic Flows, *AIAA Paper 92-2975*.
- Wagner, W.** (1992): A Convergence Proof for Bird's Direct Simulation Monte Carlo Method for the Boltzmann Equation, *Journal of Statistical Physics*, **66**, p. 1011.
- Wesseling, P.** (2001): *Principles of Computational Fluid Dynamics*, p. 569, Springer.
- Wijesinghe, H. S.; Hadjiconstantinou, N. G.** (2002): A hybrid continuum-atomistic scheme for viscous incompressible flow, *Proceedings of the 23th International Symposium on Rarefied Gas Dynamics*, pp. 907–914, Whistler, British Columbia.
- Wijesinghe, H. S.; Hadjiconstantinou, N. G.** (2004): Hybrid atomistic-continuum simulations for multiscale hydrodynamics, *International Journal on Multiscale Computational Engineering*, accepted for publishing.

**Wong, J. S.; Darmofal, D. L.; Peraire, J.** (2001): The Solution of the Compressible Euler Equations at Low Mach Numbers Using a Stabilized Finite Element Algorithm, *Computer Methods in Applied Mechanics and Engineering*, **190**, pp. 5719–5737.